Optical properties of n-doped $Ga_{1-x}Mn_xN$ epitaxial layers grown by metal-organic chemical-vapor deposition in mid and far (5–50 μm) IR range

A. B. Weerasekara, Z. G. Hu, N. Dietz, and A. G. U. Perera[a]
Department of Physics and Astronomy, Georgia State University, Atlanta, Georgia 30303

A. Asghar and M. H. Kane
School of Electrical and Computer Engineering, Georgia Institute of Technology, Atlanta, Georgia 30332

M. Strassburg
Department of Physics and Astronomy, Georgia State University, Atlanta, Georgia 30303 and School of Electrical and Computer Engineering, Georgia Institute of Technology, Atlanta, Georgia 30332

I. T. Ferguson
School of Electrical and Computer Engineering and School of Materials Science and Engineering, Georgia Institute of Technology, Atlanta, Georgia 30332

(Received 6 July 2007; accepted 5 November 2007; published 3 January 2008)

Optical properties of n-doped (Si) hexagonal $Ga_{1-x}Mn_xN$ films ($x=0.015$) grown by metal-organic chemical-vapor deposition (MOCVD) on c-plane sapphire substrates have been studied by infrared reflectance spectroscopy. The effect of free carriers on GaMnN optical phonons, namely E_1(LO) and E_1(TO), is explored. It is found that the frequency of E_1(LO) increases with increasing free carrier concentration. The absorption coefficient (α) is calculated for the 200–2000 cm^{-1} range and the maximum value of α is found to be $\sim 10^5$ cm^{-1} at a frequency of 560 cm^{-1}. With increasing free carrier concentration, the FWHM of the absorption peak increased by 35%–40% as compared to an unintentionally doped ($<1\times 10^{16}$ cm^{-3}) film. © *2008 American Vacuum Society.*
[DOI: 10.1116/1.2819259]

I. INTRODUCTION

With the development of dilute magnetic semiconductors (DMS) such as GaMnAs, InMnAs, and GaMnN, spintronic devices[1] such as spin $p-n$ diodes, spin transistors, spin detectors, spin LEDs, etc. are at the center of attention. During the past few years, $Ga_{1-x}Mn_xN$ thin films have attracted great attention in the field of semiconductor spintronics due to the theoretical prediction of high Curie temperatures[2] and experimental reports of room temperature ferromagnetism.[3] Although studies on the magnetic properties of $Ga_{1-x}Mn_xN$ are widely available,[3–7] only a few studies on the optical properties of $Ga_{1-x}Mn_xN$ epitaxial films, especially in the far infrared (FIR) and mid infrared (MIR) regions, have been reported.[5,8,9] Designing such spintronic and opto-electronic devices based on $Ga_{1-x}Mn_xN$ requires a broader understanding of optical and electrical properties of epitaxial films, which are still rare in the literature. In a recent paper, the optical properties of undoped $Ga_{1-x}Mn_xN$ expitaxial films grown by metal-organic chemical-vapor depositions (MOCVD) were presented.[8] In this study, the optical properties of n-doped (Si) $Ga_{1-x}Mn_xN$ are investigated using IR reflection spectroscopy. The focus of this article includes a study of the behavior of high frequency dielectric constant ε_∞ and optical phonon modes [E_1(TO) and E_1(LO)] in n-doped (Si) $Ga_{1-x}Mn_xN$ epitaxial films deposited on sapphire substrates and a comparison of optical properties of doped and undoped $Ga_{1-x}Mn_xN$ epitaxial films and GaN films in the IR range of 200–2000 cm^{-1} (5–50 μm). In addition, the IR absorption coefficient in the range of 200–2000 cm^{-1} (5–50 μm), which is very important for IR device development, is also discussed.

II. EXPERIMENT

Three n-doped (Si) hexagonal $Ga_{1-x}Mn_xN$ expitaxial films, denoted as 1216m (0.2×10^{18} cm^{-3}), 1218m (1.8×10^{18} cm^{-3}), and 1221m (2.1×10^{18} cm^{-3}), and one undoped hexagonal $Ga_{1-x}Mn_xN$ film, 1215m ($<1\times 10^{16}$ cm^{-3}), were used in this study. The manganese composition, x, was kept at $x=0.015$ (1.5%) for all four samples. The $Ga_{1-x}Mn_xN$ films, 1216 and 1218m, were deposited on n-GaN/GaN/AlN/sapphire templates while the $Ga_{1-x}Mn_xN$ films, 1221 and 1215m, were deposited on GaN/AlN/sapphire templates. The thicknesses of the GaN epilayer, the n-GaN epliayer, and the AlN buffer layer were $\sim$1.8 μm, $\sim$300 nm, and $\sim$20 nm. C-plane sapphire was used as the substrate material. The epilayers were deposited using a customized GaN MOCVD reactor with a vertical injection system. Ammonia, tri-methyl gallium, bis-cyclopenadienyl manganese (Cp_2Mn), and silane (SiH_4) were used as the nitrogen, gallium, manganese, and n-dopant sources, respectively, for the growth of $Ga_{1-x}Mn_xN$ films. The concentration of the incorporated Mn was controlled by the molar flow of Mn entering the reactor. Additional details of the growth pro-

[a]Electronic mail: uperera@gsu.edu

cess were reported elsewhere.[4] Near normal incidence ($\sim 8°$) IR reflection measurements at room temperature were performed over the frequency range of 200–2000 cm^{-1} (5–50 μm) using a Perkin-Elmer system 2000 fast Fourier transform infrared spectrometer (FTIR). The IR reflection spectra were taken under *s*-polarized and near normal ($\sim 8°$) incident light arrangement to minimize the effect of anisotropy of the hexagonal $Ga_{1-x}Mn_xN$ film.

The dielectric function of doped $Ga_{1-x}Mn_xN$ films in the IR region is predominantly determined by the phonon and the free carrier contributions. The phonon contribution arises from local lattice vibrations under the propagating electric field of the incident light. This can be modeled using a Lorentz oscillator. The free carrier plasma contribution is due to the interaction of free carriers with the electric field of the incidence light. It can be modeled using a classical Drude model approximation. Hence, a complete but simple model for the dielectric function of doped $Ga_{1-x}Mn_xN$ films can be presented as in Eq. (1) for IR region,[10,11]

$$\varepsilon(\omega,n) = \varepsilon_\infty\left[1 + \frac{\omega_{LO}^2 - \omega_{TO}^2}{\omega_{TO}^2 - \omega^2 - i\omega\Gamma} - \frac{\omega_p^2(n)}{\omega^2 + i\omega\gamma_p}\right], \tag{1}$$

where ε_∞ is the high-frequency dielectric constant, and ω_{LO}, ω_{TO}, and Γ are the longitudinal (LO) frequency, transverse (TO) frequency, and the broadening constant of the E_1 phonon while ω_p and γ_p are the plasma frequency and its damping constant. Moreover, this model addresses the phonon-plasmon coupling. Our recent study[8] on the optical properties of undoped $Ga_{1-x}Mn_xN$ in the IR region shows that considering only E_1 phonon modes in the dielectric model can accurately predict the experimental IR reflection spectra. Therefore, only the E_1 phonon modes (LO and TO) were considered for the lattice vibration contribution.

The transfer matrix method was used to calculate IR reflectance spectra from the multilayer structures.[12] Electric fields in each thin film layer can be calculated using the interface matrix [Eq. (2)] between the $(j-1)$th and the jth layers and the propagation matrix [Eq. (3)] in the jth layer:

$$T_{j-1,j} = \frac{1}{2\sqrt{\varepsilon_j}}\begin{bmatrix} (\sqrt{\varepsilon_j} + \sqrt{\varepsilon_{j-1}}) & (\sqrt{\varepsilon_j} - \sqrt{\varepsilon_{j-1}}) \\ (\sqrt{\varepsilon_j} - \sqrt{\varepsilon_{j-1}}) & (\sqrt{\varepsilon_j} + \sqrt{\varepsilon_{j-1}}) \end{bmatrix}, \tag{2}$$

$$D_j = \begin{bmatrix} \exp(i2\pi\sqrt{\varepsilon_j}d_j/\lambda) & 0 \\ 0 & \exp(-i2\pi\sqrt{\varepsilon_j}d_j/\lambda) \end{bmatrix}, \tag{3}$$

where ε_j is the dielectric function of the jth layer, d_j is the thickness of the jth layer, and λ is the wavelength of the incident light. Light propagation in the whole structure can be expressed by a single matrix obtained by multiplying the interface and the propagation matrices of the multilayer structure, which allows the reflectance coefficient for the whole structure to be easily calculated. A five phase model (air/$Ga_{1-x}Mn_xN$/n-GaN/GaN/sapphire) was used to model IR reflections on 1216 and 1218m while the IR reflection spectra for 1221 and 1215m were modeled using a four phase model (air/$Ga_{1-x}Mn_xN$/GaN/sapphire). Note the additional *n*-doped GaN layer in 1216 and 1218m. The effect of the AlN buffer layer on IR reflection was found to be negligible and was ignored in the fitting process since the layer thickness is very small when compared to the other layers. A nonlinear fitting algorithm, Levenberg-Marquardt,[13] was used to extract the best fit parameters for modeling the experimental IR reflection of the $Ga_{1-x}Mn_xN$. Initially, IR reflection spectra of the sapphire substrate and the sapphire/GaN template were fitted to the modeled reflection spectra to extract the parameters for the sapphire substrate and the GaN layer. Later, those parameters were fixed during the $Ga_{1-x}Mn_xN$ IR reflection fitting.

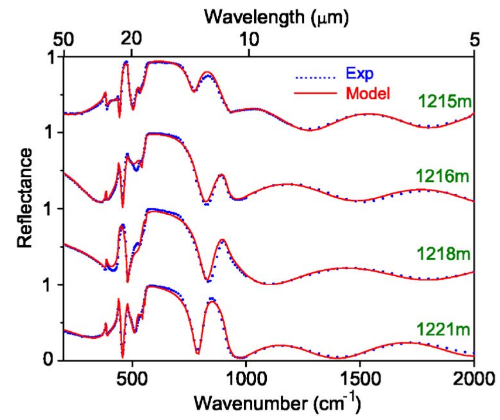

FIG. 1. Experimental infrared reflectance spectra (dotted lines) of the $Ga_{1-x}Mn_xN$ films on sapphire substrates and the best fit using Eq. (1) (solid lines). For clarity, each spectrum is successively shifted by 1.0 in the vertical direction.

III. RESULTS AND DISCUSSION

Optical constants ε_∞, ω_{LO}, ω_{TO}, Γ, ω_p, and γ_p for $Ga_{1-x}Mn_xN$ films were extracted by fitting the experimental IR reflectance spectra. The experimental and modeled IR reflection spectra from 200 to 2000 cm^{-1} (50–5 μm) are shown in Fig. 1. Parameters for doped $Ga_{1-x}Mn_xN$ films are listed in Table I along with an undoped $Ga_{1-x}Mn_xN$ film parameters for comparison. The $Ga_{1-x}Mn_xN$ film thicknesses in samples 1215, 1216, 1218, and 1221m were found to be 1765, 1252, 424, and 1335 nm, respectively. The high frequency dielectric constant, ε_∞, for *n*-doped and undoped $Ga_{1-x}Mn_xN$ films did not vary significantly and remained around 5.2. The free carrier concentration, n, was calculated using Eq. (4):

$$\omega_p = \left[\frac{ne^2}{m^*\varepsilon_\infty\varepsilon_0}\right]^{1/2}, \tag{4}$$

where ω_p is the plasma frequency and was obtained from the fitting, e is electron charge, m^* is the electron effective mass, and ε_0 is permittivity of free space. m^* was taken as $0.2m_0$ where m_0 is the free electron mass. Plasma frequencies for the three *n*-doped films, 1216, 1218, and 1221m, are 130, 380, and 422 cm^{-1}, respectively. From these plasma frequencies, the calculated free carrier concentrations for 1216, 1218, and 1221m are ~ 0.2, ~ 1.8, and $\sim 2.1 \times 10^{18}$ cm^{-3}, respectively. As previously shown, the frequency of E_1(TO)

TABLE I. Parameters obtained from the best fits of IR spectra and sample information. Sample numbers, high frequency dielectric constant (ε_∞), E_1(LO) and E_1(TO) mode frequencies, damping constant of E_1 phonon (Γ), and frequency and damping constant of the plasma oscillator (ω_p, γ_p). Free carrier concentration, n, was derived from the plasma frequency. Mn composition, x, is 1.5% for all four films. Fitting errors are given in parentheses.

Samples	ε_∞	ω_{LO} (cm^{-1})	ω_{TO} (cm^{-1})	Γ (cm^{-1})	ω_p (cm^{-1})	γ_p (cm^{-1})	n (10^{18} cm^{-3})
1215m	5.22(0.04)	745(1)	564(1)	9.6(0.3)	N/A	N/A	<0.01
1216m	5.17(0.04)	745(2)	561(1)	6.5(1.1)	130(20)	150(90)	0.2
1218m	5.20(0.10)	747(5)	563(1)	8.0(1.9)	366(24)	130(57)	1.8
1221m	5.16(0.05)	754(2)	562(1)	8.09(1.3)	407(10)	387(32)	2.1

in undoped $Ga_{1-x}Mn_xN$ shifts linearly with Mn composition[8] and was found to be at 564 cm^{-1} for 1.5% Mn concentration. However, the frequency of E_1(TO) in Si doped $Ga_{1-x}Mn_xN$ films ($0.02-2.1\times10^{18}$ cm^{-3}, $x=0.015$) was found to be slightly smaller than that of undoped $Ga_{1-x}Mn_xN$ (see Table I). A slight decrease in E_1(TO) frequency in GaN with increasing doping concentration can been seen in the work reported by Kasic *et al.*;[10] however, Li *et al.*[14] have seen a slight increase in E_1(TO) frequency with increasing doping concentration in GaN. This can be due to the extra strain in the lattice introduced by Si dopants and different film thicknesses. The E_1(LO) frequencies for both undoped (1215m, $<1\times10^{16}$ cm^{-3}) and low doped (1216m, 0.2×10^{18} cm^{-3}) $Ga_{1-x}Mn_xN$ films are at $\sim$745 cm^{-1}, which is slightly higher than the reported values for GaN: 742.1, 738.4, and 737.5 cm^{-1} by Kasic and Schubert,[10] and 741 cm^{-1} by Harima.[15] The E_1(LO) frequencies for samples 1218 and 1221m shifted to higher frequencies due to the stronger LO-phonon and plasmon coupling (LPP). When the plasma frequency gets closer to the LO-phonon frequency, the coupling gets stronger and therefore LO frequency shifts to higher frequency.[11]

The coupling of longitudinal optical phonons [E_1(LO) and A_1(LO)] and plasmons, LPP modes, is expected when free carriers are present in the material and is stronger when the plasma frequency, ω_p, is near the longitudinal optical phonon (LO) frequencies. The behaviors of the couple modes between E_1(LO) and the plasmon (E_1-LPP) for n-doped films 1216, 1218, and 1221m are shown in Figs. 2(a)–2(c), respectively. Frequencies of E_1-LPP$^+$ are 750, 800, and 810 cm^{-1} while frequencies of E_1-LPP$^-$ are 85, 260, and 255 cm^{-1} for samples 1216, 1218, and 1221m, respectively. The LPP mode frequency can be theoretically calculated by setting the dielectric function [Eq. (1)] to zero in the limit of zero damping and is given as follows:

$$\omega_\pm = \frac{\omega_{LO}^2+\omega_p^2}{2} \pm \left[\frac{(\omega_{LO}^2+\omega_p^2)^2}{2} - \omega_p^2\omega_{TO}^2\right]^{1/2}. \quad (5)$$

Figure 2(d) shows the theoretically predicted E_1-LPP mode behavior and experimentally deduced E_1-LPP frequencies as free carrier concentration increases. Generally, the LPP$^+$ mode reaches ω_{LO} and the LPP$^-$ mode reaches zero as the free carrier concentration reaches zero [see the two solid

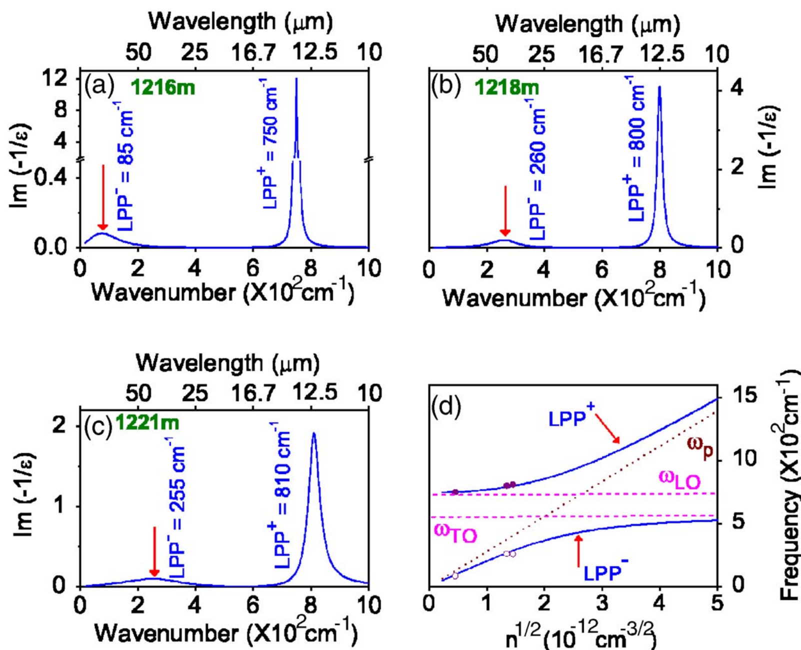

FIG. 2. Im($-1/\varepsilon$) as function of frequency is shown for three doped $Ga_xMn_{1-x}N$ samples: (a) 1216m, (b) 1218m, and (c) 1221m. Plasmon and phonon coupling modes, E_1-LPP$^+$ and E_1-LPP$^-$ are clearly visible. A comparison of experimentally derived and theoretically predicted E_1-LPP mode behavior with square root of free carrier concentration is shown in (d). Solid lines: theoretically predicted behavior of E_1-LPP$^+$ and E_1-LPP$^-$, Solid dots and white circles: experimentally obtained E_1-LPP mode values, Dashed lines: ω_{TO} and ω_{LO}. Dotted line: ω_p variation.

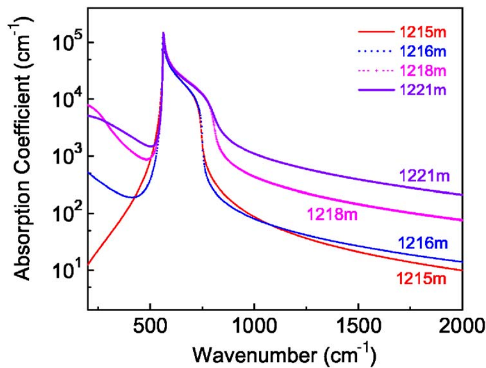

FIG. 3. The derived absorption coefficients, α for all four $Ga_{1-x}Mn_xN$ films in 200–2000 cm^{-1} (50–10 μm). The absorption coefficient reaches its maximum at 550 cm^{-1}. The width of the absorption peak has increased by 35%–40% in higher doped films ($>1\times10^{18}$ cm^{-3}).

lines in Fig. 2(d)]. Therefore, the LPP^+ mode shows ω_{TO} phononlike behavior at low doping. As the free carrier concentration increases, the LPP^+ mode approaches ω_p while the LPP^- mode approaches ω_{TO} (see the two solid lines). Therefore, the LPP^+ mode shows plasmonlike behavior for higher doping concentrations.

A knowledge of IR absorption coefficient of materials, α, is important for designing infrared detectors and α can be calculated using Eq. (6):

$$\alpha = \frac{4\pi \, \mathrm{Im}(\sqrt{\varepsilon})}{\lambda}, \qquad (6)$$

where $\mathrm{Im}(\sqrt{\varepsilon})$ is the imaginary part of the square root of the dielectric function and λ is the wavelength. The calculated absorption coefficients for all four films are shown in Fig. 3 in the 200–2000 cm^{-1} range (5–50 μm). The absorption coefficient peaks in the GaN Reststrahlen band and reaches its maximum, 1×10^5 cm^{-1}, around the frequency 560 cm^{-1}. The absorption peak gets broader with increasing free carrier concentration. For highly doped $Ga_{1-x}Mn_xN$ films, the line width of the absorption peak has increased by about 35%–40% with respect to undoped or low doped $Ga_{1-x}Mn_xN$ films. This broadening is due to the LPP^+ mode shifting to higher frequency with increasing doping. At frequency 200 cm^{-1} (50 μm), absorption has increased from 12 cm^{-1} to roughly 7500 cm^{-1} as the free carrier concentration was increased to 2.1×10^{18} cm^{-3} from undoped ($<1\times10^{16}$ cm^{-3}). The increase in α at wave number 200 cm^{-1} is an advantage for far infrared detectors. In addition, in the short wavelength region (1000–2000 cm^{-1}), α has increased by a factor of 5, at least, the highest doped $Ga_{1-x}Mn_xN$ film. In general, α increases with increasing free carrier concentration.

IV. CONCLUSIONS

The high frequency dielectric constant, ε_∞, and optical phonon modes, E_1(LO) and E_1(TO), were investigated. High frequency dielectric constant, ε_∞, in *n*-doped $Ga_{0.985}Mn_{0.015}N$ films is between 5.2 and 5.3, which is close to the reported values of undoped $Ga_{1-x}Mn_xN$ (Ref. 8) and GaN.[15,16] The frequencies of E_1(TO) of doped and undoped $Ga_{0.985}Mn_{0.015}N$ films do not show a significant difference, whereas E_1(LO) frequency increases with increasing free carrier concentrations for the investigated range of 2×10^{17} to 3×10^{18} cm^{-3}.

ACKNOWLEDGMENTS

This work was supported in part by the U. S. NSF under Grant Nos. ECS-0553051 and GSU-RPE. The authors acknowledge N. Li for Hall measurements.

[1]S. A. Wolf, D. D. Awschalom, R. A. Buhrman, J. M. Daughton, S. von Molnar, M. L. Roukes, A. Y. Chtchelkanova, and D. M. Treger, Science **294**, 1488 (2001).
[2]T. Dietl, H. Ohno, F. Matsukura, J. Cibert, and D. Ferrand, Science **287**, 1019 (2000).
[3]G. T. Thaler *et al.*, Appl. Phys. Lett. **80**, 3964 (2002).
[4]M. H. Kane *et al.*, Semicond. Sci. Technol. **20**, L5 (2005).
[5]M. Zajac *et al.*, Appl. Phys. Lett. **78**, 1276 (2001).
[6]S. Marcet, D. Ferrand, S. Kuroda, E. Gheeraert, R. M. Galera, J. Cibert, and H. Mariette, Mater. Sci. Eng., B **126**, 240 (2006).
[7]M. L. Reed, M. J. Reed, M. O. Luen, E. A. Berkman, F. E. Arkun, and S. M. Bedair, Phys. Status Solidi C **2**, 2403 (2005).
[8]Z. G. Hu, M. Strassburg, A. Weerasekara, N. Dietz, A. G. U. Perera, M. H. Kane, A. Asghar, and I. T. Ferguson, Appl. Phys. Lett. **88**, 061914 (2006).
[9]Z. G. Hu, A. B. Weerasekara, N. Dietz, A. G. U. Perera, M. Strassburg, M. H. Kane, A. Asghar, and I. T. Ferguson, Phys. Rev. B **75**, 205320 (2007).
[10]A. Kasic, M. Schubert, S. Einfeldt, and D. Hommel, Phys. Rev. B **62**, 7365 (2000).
[11]T. Kozawa, T. Kachi, H. Kano, Y. Taga, M. Hashimoto, N. Koide, and K. Manabe, J. Appl. Phys. **75**, 1098 (1994).
[12]C. C. Katsidis and D. I. Siapkas, Appl. Opt. **41**, 3978 (2002).
[13]W. H. Press, S. A. Teukolsky, W. T. Vetterling, and B. P. Flannery, *Numerical Recipes in C: The Art of Scientific Computing* (Cambridge U. P., Cambridge, MA, 1992).
[14]Z.-F. Li *et al.*, J. Appl. Phys. **86**, 2691 (1999).
[15]H. Harima, J. Phys.: Condens. Matter **14**, R967 (2002).
[16]A. S. Barker, Jr. and M. Iiegems, Phys. Rev. B **7**, 743 (1973).